Simulated and Reconstructed Temperature in China since 1550 AD

Jian Liu[1], Hans von Storch[2], Eduardo Zorita[2],
Xing Chen[3,1], and Sumin Wang[1]

1. Nanjing Institute of Geography and Limnology, Chinese Academy of Sciences, Nanjing 210008, P.R.China

2. Institute for Coastal Research, GKSS Research Center, 21502 Geesthacht, Germany

3. Department of Atmospheric Sciences, Nanjing University, Nanjing 210093, P.R.China

Abstract

In this paper, reconstructed decadal mean temperature anomaly series of 8 regions of China are compared to those generated in two multi-century simulations with a climate model, which was forced with time variable volcanic aerosols, solar output and atmospheric greenhouse gas concentrations. The two model simulations are rather similar but do exhibit some differences. Both the reconstructed and simulated developments of the temperature exhibit a "hockey-stick" pattern, with a marked increase of temperatures since the beginning of the twentieth century. The variations of time scales of a few decades are, however, mostly dissimilar in the historical and proxy-based account and also in the model data.

An attempt is made to assess whether the warming during the twentieth century is within the range of "normal'' variations related to solar and internal dynamical influences. It is found that the reconstructed data are well above the pre-industrial noise level of temperature fluctuations during most of the twentieth century. Within the adopted framework, only the increased greenhouse gas concentrations can account for these significantly elevated temperatures.

Key words: China, climate, temperature, climate model, climate change, detection

Introduction

Research of climate change since the Little Ice Age (LIA, 1550-1850AD) has received extensive attention in China. Widespread and severe famine and serious social turmoil have occurred in China during the LIA (Xu, 1998). Also, the warm conditions after the LIA had great impact on human life and the national economy (Yang, et al. 2002). Because of this broad

interest, the climate of China during the last 2000 years has been reconstructed by Chinese scientists, in particular temperature and precipitation since LIA with a variety of proxy data, such as historical documents, tree rings, ice cores, lake warves, archaeological materials, etc. (Wang et al., 1998; Wang and Gong, 2000; Liu and Cai, 2002; Liu and Ma, 1999, Liu and Shao, 2002, Zheng and Zheng, 1993; Yao et al. 1996).

Recently, two long-term climatic simulation experiments have been done by a consortium of scientists from the Institute for Coastal Research, the GKSS Research Centre and other institutions. The first run, named "Christoph Columbus" (CC) was run over 535 years beginning in 1450, and is described in some detail by Zorita et al. (2003). The second run, named "Erik den Røde" (EdR), was begun in 900 and ran over 1100 years. Both simulations were done with the same ECHO-G climate model with, however, different code versions adapted to different computer systems. Reconstructed time series of the radiative effect of the presence of volcanic aerosols, greenhouse gases in the atmosphere as well as variable solar output were used as forcing (see below). The modeling results reveal global and regional patterns of natural and anthropogenic climate change, which have some similarities with the observational record (Zinke et al., 2004, De Zolt et al., 2003). The purpose of the present study is to compare these simulated data with observational evidence for the territory of China, and to interpret the recent changes of Chinese temperatures in the context of the forced climate model.

In Section 2 we briefly introduce the reconstructed temperature data used in this comparison, and in Section 3 the simulations are sketched. In Section 4 the simulated and reconstructed historical temperature anomalies are compared. In Section 5, the warming in the last century is identified as being beyond the range of variations related to natural and internal causes, and in Section 6 the paper is concluded with a brief discussion.

Reconstructed temperature from China

Continental monsoon dynamics with complicated seasonal patterns are the major characteristics of China's present climate. The northerly monsoon prevails in winter, the southerly in summer, and the four seasons are very distinct. The season with most of rainfall is summer. From September to April each year, the cold and dry winter monsoon blows from the Siberia and Mongolia plateau to the mainland of China and weakens gradually from northwest to southeast, causing the cold and dry climatic state with a very large difference in temperature. The length of the wet summer monsoon control is shorter, from April to September. The warm and wet summer monsoon blows from the western Pacific and Indian Oceans, causing a state with high temperature and much rain, with little difference in temperature from north to south.

China can be divided into 10 districts (Wang at al., 1998a), which are relatively homogeneous in terms of temperature, precipitation and growing season. These are northeast China, north China, east China, the middle of China, south China, southeast China, southwest China, northwest China, the Xinjiang region and the Tibet region. With proxy data from historical documents, tree rings and ice cores available, reconstructions of the temperature series have been made for all these regions, except regions of northeast China and Xinjiang region (Figure 1). The reconstructions of 10-year mean temperature anomalies are based on proxies, such as temperature index, tree ring width and density, $\delta^{18}O$ of ice cores, via statistical techniques which rely on establishing empirical relationships between modern observations and environments (Wang et al., 1998a). The proxy data and time series length of the reconstructed temperature anomalies can be found in Table 1. They are anomalies relative to 1880-1979.

The reconstructions have been compared with the empirical evidence available from the past century. Unfortunately, this evidence is very uncertain. One analysis of decadal mean temperatures has been prepared by Wang et al. (1998b), who used three kinds of data: 1951-1996 CMA's monthly temperature series from 165 stations for whole China, 1911-1950 CMA's temperature grade diagram series for 139 stations of China, and 1880-1910 documentary, ice core and tree-ring data. On the other hand, Jones et al. (1999) made an attempt to reconstruct Chinese temperatures from 1856 to 1998 AD. This reconstruction is also rather uncertain, in particular for before 1949 (Jones, pers. comm.). Both reconstructions deviate markedly from each other also in recent decades, as is demonstrated in Figure 2.

The fit of the historical data and the "observed" data is facilitated by using data from the Wang et al. analysis (1998b). Unfortunately, we have no access to the original analyses by Wang et al. (1998b) except for region 3. Also, robust measures of skill for this reconstruction are not available either, and it seems plausible that the very good fit shown in Figure 2 is the result of overfitting. Unfortunately we have no means to assess which of the two reconstructions (Wang and Jones) is more skilful, nor to do our own analysis with the raw data. Therefore we have to rely on the published results, even if we have some doubts about the methodology.

We therefore adopt the pragmatic, and admittedly to some degree questionable standpoint, that Wang's reconstruction is essentially valid on time scales of several decades, e.g., 5-decade running means. The root mean square difference between the 5-decade running means given by the historical reconstruction (based upon historical evidence and geoscientific proxies, fitted to the unavailable Wang et al. (1998b) data set) and Jones et al. (1999) varies between 0.13ºK and 0.36ºK in the eight regions, and averaged 0.24ºK for all regions. We consider this number a crude but educated estimate of the inherent uncertainty of the historical temperature variations in China on the time scale of 50 years.

The time-averaged time series are shown in Figure 3. They all share a marked warming since about 1900 by 0.5ºK and more. In 7 out of the 8 regions, the last decades are associated with a cooling, and only in region 4 is the warming continuing. Before 1900 the temperatures vary very differently in the 8 regions. In particular region 7 and 8, for which the estimates are not based upon on historical data but on geoscientific proxy data (Table 1), which exhibit rather strong negative temperature swings, with additional temperature differences in the warmer regions by 0.5ºK. It is not entirely plausible that the temperature variations are so unconnected even on time scales of 50 and more years. In fact, the variations simulated in the climate model are much more uniform, but it is unclear if this is a realistic property or not.

Table 1. Proxy data and reconstructed series length of 8 regions. (Wang et al., 1998a)

No.	Region	Proxy data	Length
1	North China	Historical materials	1380-1990
2	East China	Historical materials	1380-1990
3	South China	Historical materials	1500-1990
4	Southeast China	Historical materials	1500-1990
5	Central China	Historical materials	1470-1990
6	Southwest China	Historical materials	1500-1990
7	Northwest China	Ice cores	1000-1990
8	Tibet	Tree rings	1000-1990

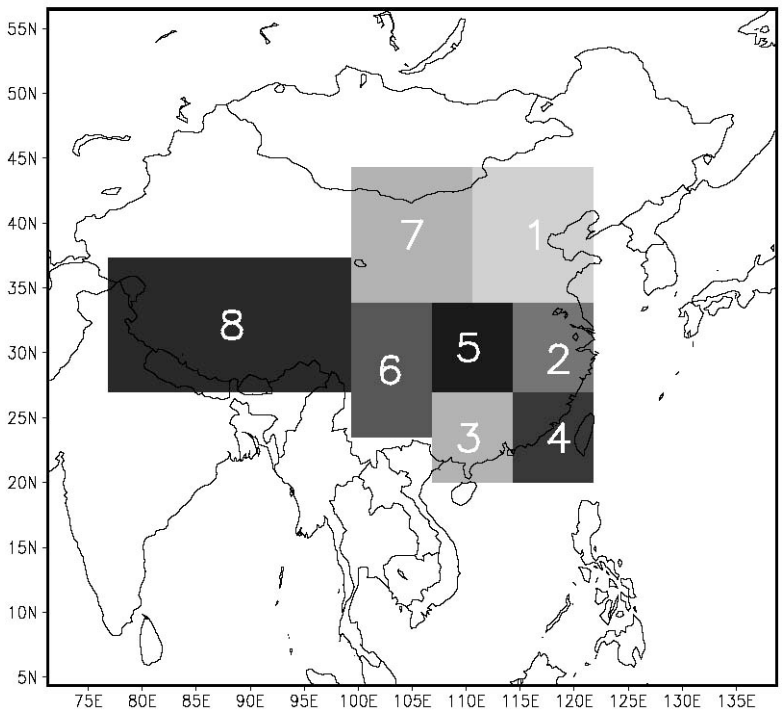

Fig. 1. Regions of China with reconstructed temperature series

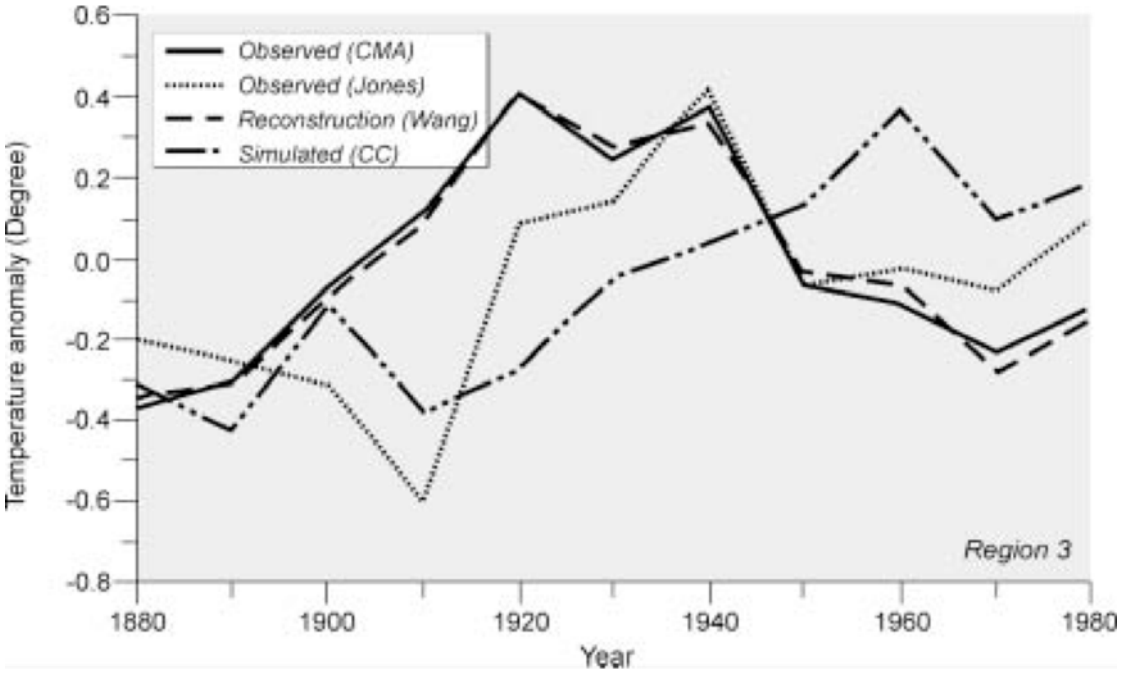

Fig. 2. Conflicting assessment of decadal mean temperature fluctuations in region 3 of China – according to the Wang et al. (1998b) analysis of mainly instrumental data (CMA data), Jones et al. (1999), the historical reconstruction by Wang et al. (1998a), and the CC simulation with ECHO-G. The decades are labeled by the first year of a decade, e.g., 1920 stands for the years 1920-1929.

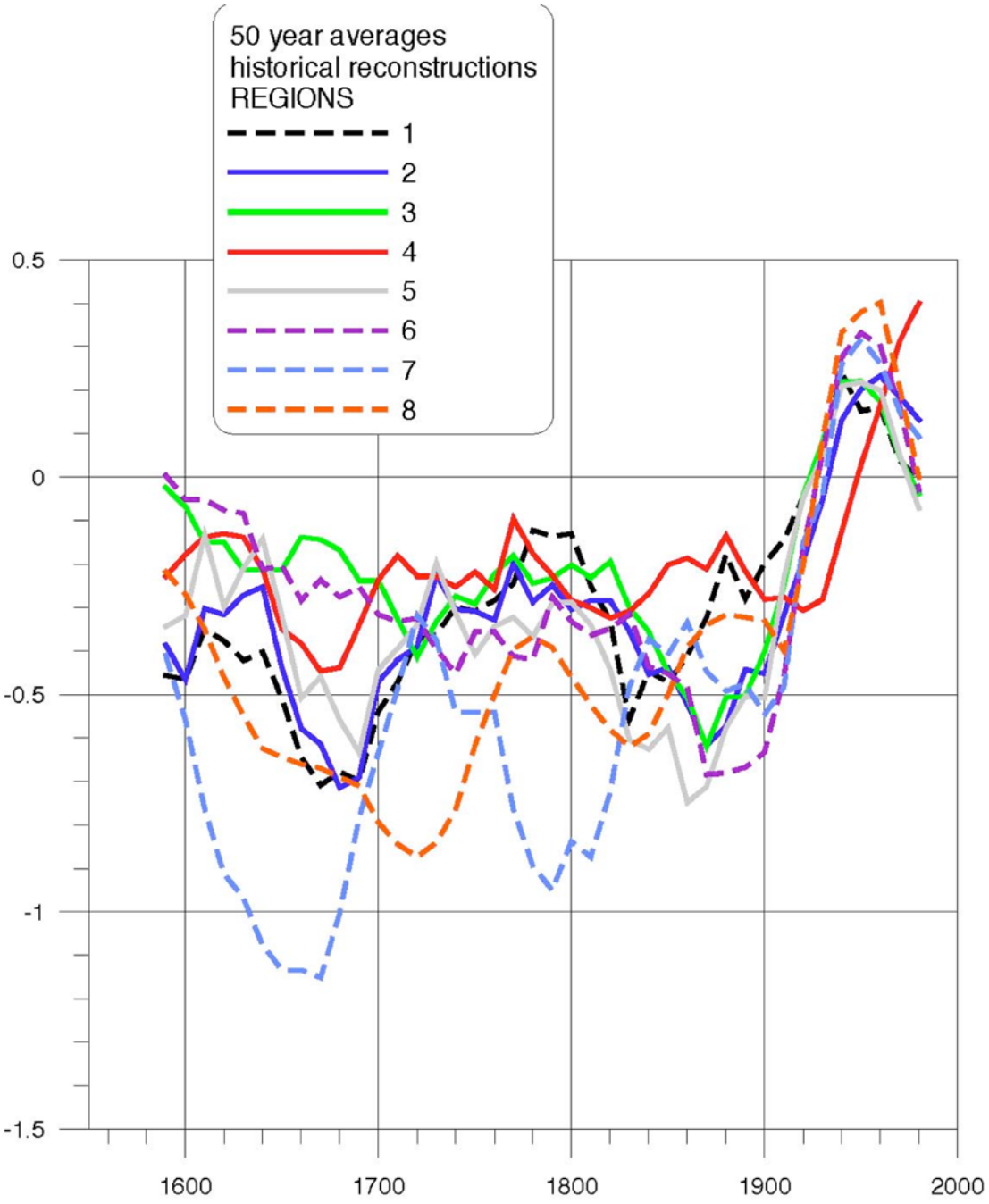

Fig. 3. Time series of reconstructed, temporarily smoothed mean temperatures for the 8 regions shown in Figure 1. A running mean filter, averaging 5 consecutive decadal means is applied so that effectively 50-year means are shown.

ECHO-G simulations, 1550-2000

Two multi-century integrations have been performed with the state-of-the-art climate model ECHO-G, which is a combination from the ocean model HOPE-G in T42 resolution and the atmospheric model ECHAM4 in T30 resolution, both developed at the MPI in Hamburg

(Legutke and Voss, 1999). Two runs, named “Christoph Columbus” (CC) and “Erik den Røde” (EdR) were executed, one over 535 years and another over 1100 years. The runs were exposed to time-variable external forcing related to solar and volcanic activity and changing atmospheric concentrations of greenhouse gases. The CO_2 and methane atmospheric concentrations were derived from air trapped in Antarctic ice cores (Blunier et al., 1995; Etheridge et al., 1996). The variations of solar output and the influence of volcanic aerosols on the radiative forcing were derived from the number of sunspots after 1600 AD and concentrations of cosmogenic isotopes in the atmosphere before 1600 AD (Crowley, 2000). The forcing due to volcanic aerosols was estimated from concentrations of sulphuric compounds in different ice cores, located mainly over Greenland. These forcing factors were then translated to effective variations of the solar constant in the General Circulation Model (GCM) taking into account the corresponding geometric factors and the mean earth albedo. Changing the loading of industrial aerosols has not been incorporated in the simulation.

In the following we consider only the time simulated in both runs, namely 1550 to today. For this time Figure 4 shows the history of the effective solar activity, greenhouse gas and volcanic-aerosol concentrations used to force the model. The global mean near-surface temperature is also shown.

The CC model integration was started in the year 1465 AD with the forcing conditions of 1990, and slowly driven in a 30-year transition period to the corresponding solar, volcanic-aerosol and greenhouse gas concentrations estimated for 1500 AD. The model attained an equilibrated state in about the model year 1550. The EdR simulation was started in the year 900, and the model attained its new equilibrium within the first 100 years of the integration.

The CC simulation is described in some detail by Zorita et al. (2003). Its consistency with observational evidence during the Late Maunder Minimum is described by Zinke et al. (2004), and the relationship between forcing on the one side, and the NAO and European temperature on the other side by de Zolt et al. (2003). Aspects of the EdR run are presented in González-Ruoco et al. (2004). The material presented in the following is demonstrating that the temperatures in China simulated in the two runs are rather similar, even though the period up to about 1700 EdR in some regions seems to be systematically cooler than CC.

The simulated data are available on a grid with about 300 km mesh size. The data are spatially averaged to obtain spatial mean values for the eight larger boxes shown in Figure 1.

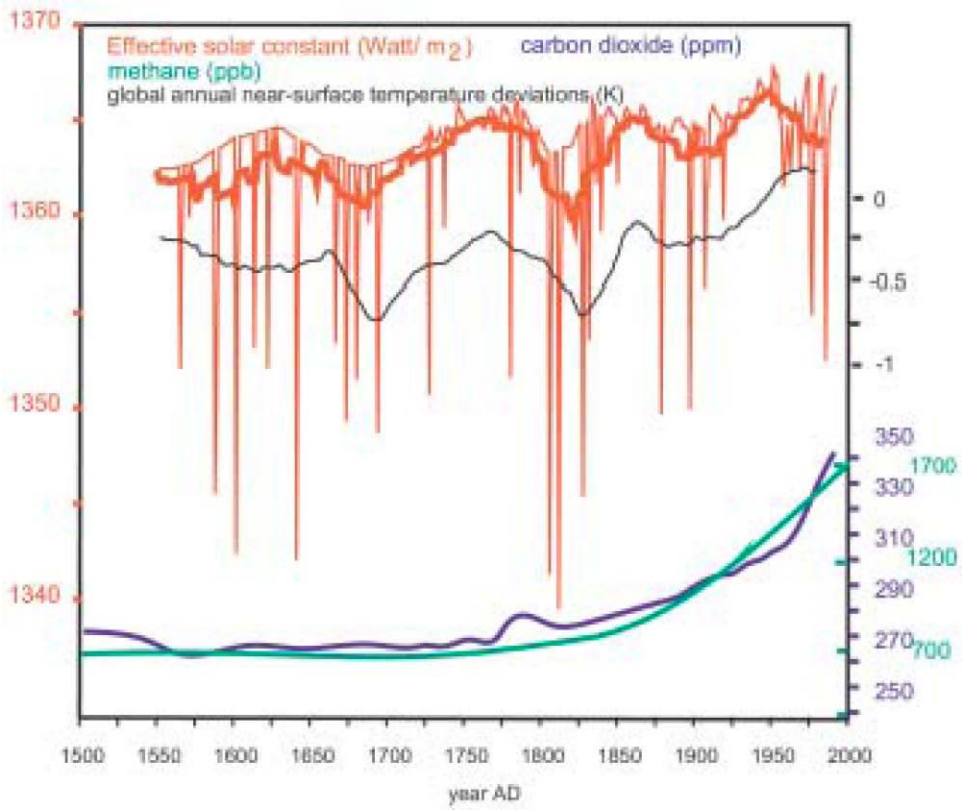

Fig. 4. Time series of simulated global mean temperature (black) in the CC simulation, of atmospheric methane and carbon dioxide concentration and effective solar constant (red), mimicking the presence of volcanic aerosols and a variable solar output used in both CC and EdR.

Comparisons between modelling results and reconstructions

All data are anomalies relative to the 10-decades (1880-1889, 1890-1899, … 1970-1979) mean. The decades are labeled by the first year, i.e., 1980 represents the years 1980-89.

We first examine the past century, because during that time the temperature estimates are based mostly on direct observations. During that time we consider decadal (10 year mean) data. In the second step, we consider the longer perspective, when only the reconstruction by Wang et al. (1998a) is available.

Previous analyses (de Zolt et al., 2003) have shown that the solar and volcanic forcing is not strong enough to imprint a strong signal on time scales of years to a few decades. Therefore, we limit our comparison to multi-decadal time scales, specifically to 5-decade running mean values (i.e., averages of 5 consecutive 10 year means). It is hoped that this smoothing also will overcome in part the inherent uncertainty of this reconstruction.

Comparison with instrumental data, 1880/1920-1979

Here we compare decadal mean temperatures for the eight boxes as simulated in the model, and as estimated from historical and geoscientific evidence (Wang et al., 1998a).

The bias between the reconstructed and simulated box-mean temperatures varies between 0.07ºK and -0.15ºK, which is, however, considerably less than the systematic difference between

Wang's estimate and Jones' estimate of 0.16ºK and -0.34ºK. For the root mean square error a similar result is found. The rmse between Wang's estimate and the simulated data is on average 0.30ºK, with a maximum value of 0.34ºK, while the two estimates differ by 0.45ºK on average, and a maximum value of 0.58ºK. Thus the difference between model and reconstruction seems insignificant when compared with the inherent uncertainty of the historical reconstructions.

Since 1920 the Jones instrumental data have relatively few gaps. Therefore, we compare for this time the variances as given by Wang's reconstruction, the Jones reconstruction, and the model output (Table 2). The simulated temperature variations are usually similar to Jones' data, with the largest difference in region 8, the Tibetan region, where the model simulates a variance up to four times the variance deduced from instrumental observations. In case of the Wang's reconstructed data, the variance is larger than the instrumental variance in 6 out of 8 cases, which is surprising insofar as the reconstructed data are derived from a regression, which underestimates variance. The largest difference is again found for the Tibetan region, but this time the factor amounts to fifteen. Again, the simulated data are consistent with the observational evidence, if we use the discrepancy between the two reconstructions as a measure of uncertainty.

We will later see that this consistency of the model data is mainly due to the strong warming trend in the past century, which is well captured by all three data sets, Wang's reconstruction and the two model simulations.

Table 2. Variances for the 8 regions since 1920 (10 year mean values)

Region	1	2	3	4	5	6	7	8
reconstructed	0.15	0.05	0.07	0.08	0.10	0.17	0.20	0.30
CC simulated	0.15	0.05	0.04	0.05	0.05	0.08	0.11	0.08
EdR simulated	0.14	0.06	0.02	0.02	0.03	0.04	0.05	0.03
Jones' estimation	0.20	0.07	0.04	0.06	0.06	0.05	0.08	0.02

Comparison of reconstructed and simulated data, 1550-2000

The 50-year running mean temperatures for the eight regions (Figure 1) as reconstructed by Wang et al. (1998a) and as simulated by the two ECHO-G runs CC and EdR are shown in Figure 5. The inherent uncertainty of the reconstructions, as estimated from the root mean square difference between Wang et al.'s (1998a) analysis of twentieth century temperature variations and Jones et al.'s (1999) analysis, is shown as well. Note that the rmse is the expected mean error, i.e., in about half the time, the error would be larger than the rmse, and in the other half smaller. Thus it is a much less stringent error margin than a 2σ confidence band.

In all cases, the warming trend since about 1900 is shared by both the reconstructed temperatures and the simulated changes. In all 8 regions, both simulations warm with a rate of about 0.4-1.1ºK/100a, whereas in Wang et al.'s reconstructions the warming is considerably weaker, -0.05 – 0.4ºK/100a, which may be due to a significant cooling caused by the emissions of industrial aerosols, which is not accounted for in the GCM simulations. An exception is region 4, in SE China, where the reconstructions reveal a heating of 1.3ºK/100a, and the GCM runs 0.5 and 0.8ºK/100a.

In the pre-industrial time (1590-1910), the GCM simulates temperatures lower than Wang's estimates. In particular in the regions 1, 2, 5 and 6, the differences are larger than the

rmse. Only in the regions 4 (SE China) and 8 (Tibet) do the simulated temperatures vary within plus/minus one rmse. In case of Tibet, the coincidence between the GCM and the proxy data is excellent. Also, the development in the Northwest, in region 7, is similar, even if the low-frequency variations are different. In the GCM world, temperatures vary around a level of -0.5ºK and less, while the reconstructed temperatures vary around a level of -0.3ºK or decline from a value close in 1550 to zero to a minimum in the late nineteenth century (regions 3 and 6 in Central and Southern China).

In general, the decadal variations are dissimilar in the reconstructed data and in the simulated data, even though the data are already heavily smoothed with a 5-decade running mean filter. The correlations between the reconstructed data and the CC-simulation for the entire period, 1590-1980, is positive (0.47 – 0.84), but these high values are essentially reflecting the presence of the hockey-stick pattern. If the two periods, pre-industrial 1590-1910 and industrial 1920-1980 are considered separately, the correlations become much smaller, namely -0.32 (region 6) to 0.72 (region 8) for the pre-industrial times, and -0.17 (region 1) to 0.32 (region 7) in modern times. (Because of the heavy serial correlation in the data, the determination of significance levels is not meaningful.)

Interestingly, the simulated curves are among themselves rather similar, quite differently from the large region-to-region variations displayed in Figure 3 for Wang's reconstruction.

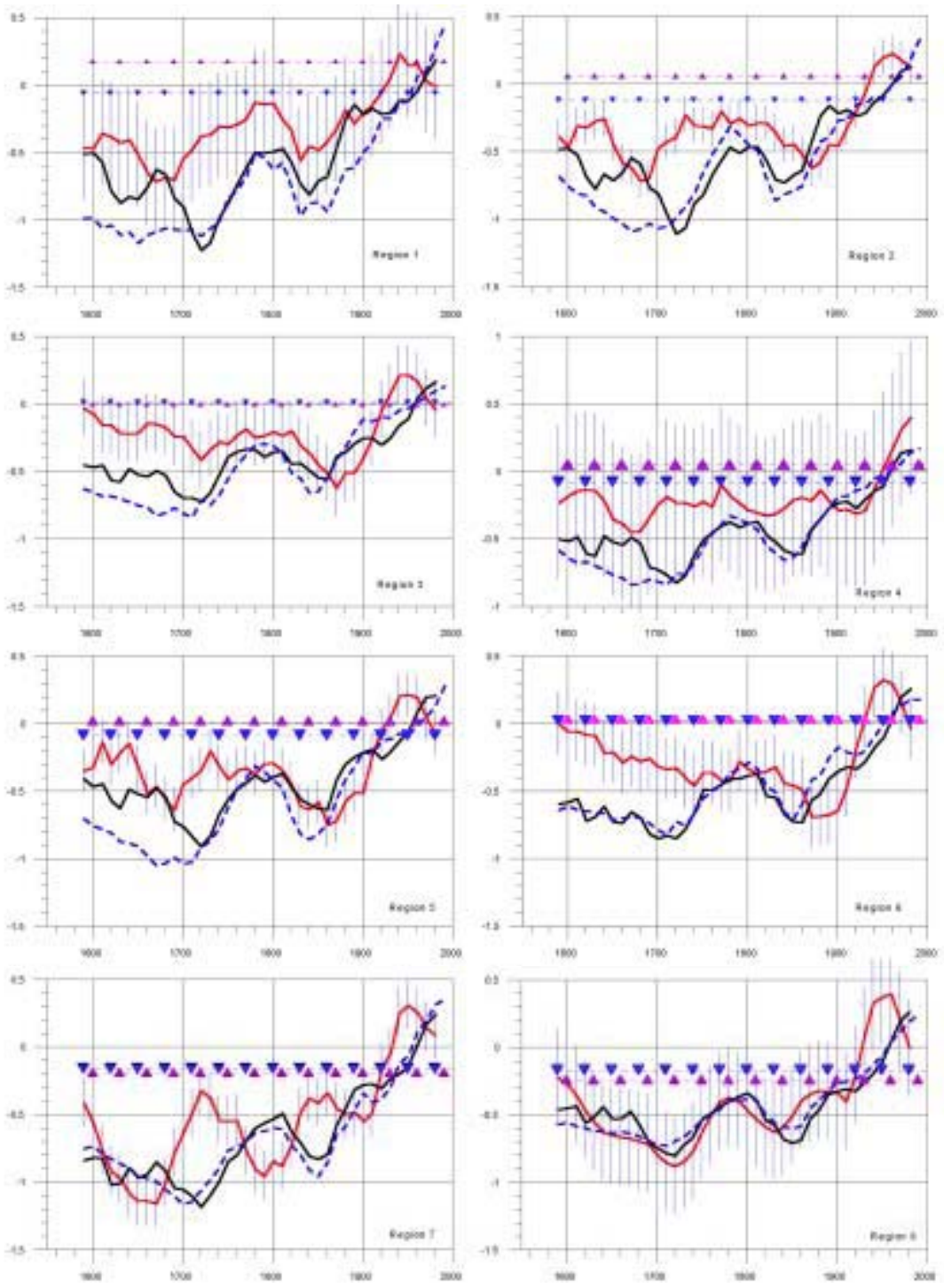

Fig. 5. Comparisons of reconstructed (red) and simulated (black: CC; blue-dashed: EdR) 5-decade running mean temperature anomaly series for 8 regions of China as given in Figure 1. The uncertainty (vertical hatching) of the reconstructed temperature variations (Wang et al., 1998) is estimated by the rmse between the reconstructed values by Wang et al (1998) and those obtained by Jones et al. (1999) since 1880. The horizontal lines with triangles indicate thresholds estimated to represent the expected range of natural variations, as estimated from Wang et al.'s reconstructions (downward triangles) and as estimated for the CC simulation (upward triangles). The 5-decade running means are labeled by the last decade, e.g., 1980 refers to 1940-1989.

EOF analysis

An EOF analysis is used to determine the joint spatial variability of the 5-decade running mean temperature for the entire time period 1590-1980. The EOFs are normalized so that the time series have a standard deviation of one, so that the magnitude of the signals is given by the patterns.

Not unexpectedly is one EOF enough to explain the bulk of the variations, namely 86% in the case of the historical reconstruction, and 99% for the two GCM data sets (Table 3). In case of the historical data, two more EOFs carry a noteworthy amount of variance, namely 5% each. As already mentioned, the synchronicity in the reconstructed data is weaker than in the GCM data (cf. Figure 5). It is unclear if this greater spatial variability (or, in other words, the larger degrees of freedom) is reflecting real temperature variations, or if it is due to the insufficiencies of the reconstruction process.

The EOF is describing a synchronous warming, or cooling, in all eight regions. The loadings in the GCM EOF are higher than in the reconstructed data EOF. This is to some extent due to the fact that less variance is described, but it is also reflecting the fact that large swings in the simulated temperature, for instance in the early eighteenth century, are absent in the reconstructed data. Again, the similarity is best in case of Tibet (region 8).

The time series associated with the first EOF modes of simulated and reconstructed data is shown in Figure 6. The correlation coefficient of these two series is 0.80. The overall similarity is remarkably large, in particular with respect to the century-scale changes, but with time scales shorter than a century, the time series differ substantially. Again the hockey-stick pattern clearly emerges. Note that the similarity in the range of variation is caused by the normalization of the EOFs.

Table 3. First EOF of reconstructed and simulated temperature in the eight regions. Prior to the EOF analysis, the data are smoothed with a running 5-decade filter. The EOFs are normalized so that the time coefficients (Figure 6) have a standard deviation of 1.

Region	1	2	3	4	5	6	7	8	Described variance (%)
reconstructed	0.36	0.38	0.25	0.24	0.38	0.31	0.63	0.53	0.86
Christoph Columbus	0.65	0.59	0.44	0.48	0.50	0.56	0.74	0.50	0.99
Erik the Red	0.82	0.70	0.54	0.55	0.67	0.53	0.75	0.50	0.99

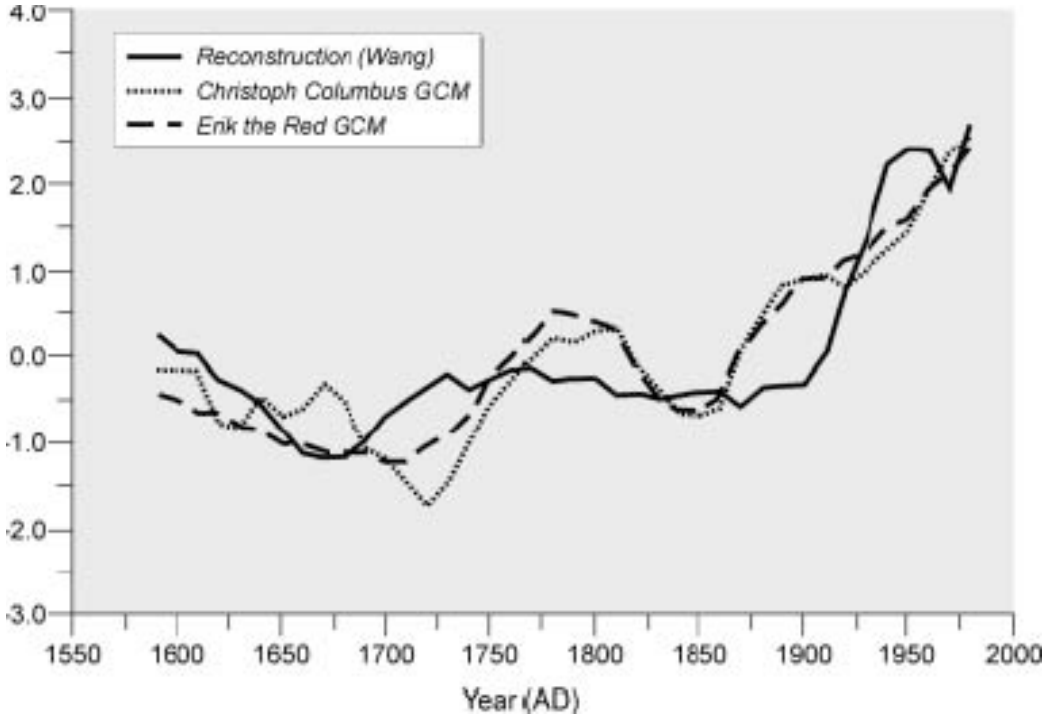

Fig. 6. Time series of the first EOF coefficients of 5-decade running mean simulated and reconstructed temperature. Note that the EOFs are normalized to standard deviation 1, so that the patterns (in Table 4) carry different magnitudes of variations. The 5-decade running mean values are labeled by the last considered decade, so that 1970 refers 1930-1979.

Assessment of the warming during the last century

The similarity of the century-scale variations in the reconstruction and in the GCM output is remarkable. The main feature of the similarity is the relatively stationary conditions until about 1900, on top of which significant decade-to-decade variations are taking place. In the GCM, these variations are related to changing forcing conditions, as displayed in Figure 4. The variations in volcanic activity contribute mostly to variations that extend only over a few years. The solar activity contributes to variations on all time scales, but the dominant signal is exerted by the increasing greenhouse gas concentrations in the twentieth century.

The question is if the reconstructed record may be interpreted similarly. This is the "detection and attribution" problem (Hasselmann, 1979; Hegerl et al., 1997; Zwiers, 1999). That is, one has first to demonstrate that the recent warming is beyond the variations one would expect from "natural variations", i.e. variations prior to 1910 due to natural and internal causes. Next, one has to demonstrate that the recent decades warming trend is consistent with the simulated response to the given forcing, i.e., to the forcing spectrum given in Figure 4.

Detection

To accomplish this, we first determine the variability of the smoothed temperature time series displayed in Figure 5 during pre-industrial times, and compare these with the changes which have taken place in the twentieth century. In Table 4, the mean value of Wang's reconstruction for 1590-1910 is listed together with the standard deviations for that time in

Wang's reconstruction, as well as in the two simulations. We consider this period of 1590-1910 as "pre-industrial time", which is not significantly affected by anthropogenic factors.

The level of variability during pre-industrial time is mostly consistent in the reconstructions and in the GCM simulations, even though there are sometimes larger differences. We consider a temperature above the range of "normal" variations, when it is larger than the mean plus two standard deviations. This "pre-industrial" noise level, as given by the mean value derived from the reconstructions plus 2 standard deviations, taken from either the reconstructions or from the CC simulations, is displayed in Figure 5 by horizontal lines marked with triangles.

Table 4. Characteristics of 5-decade running mean temperature during the "pre-industrial time" (1590-1910) in the eight Chinese regions. Wang et al.'s reconstruction (mean and standard deviation) is shown in the top two rows. GCM simulations CC and EdR (standard deviations) are shown in the bottom two rows.

Parameter	Data	1	2	3	4	5	6	7	8
time mean	Wang et al. reconstruction	-0.38	-0.40	-0.27	-0.24	-0.41	-0.34	-0.68	-0.53
standard deviation	Wang et al. reconstruction	0.16	0.14	0.14	0.08	0.16	0.18	0.26	0.18
standard deviation	CC GCM	0.27	0.23	0.13	0.15	0.17	0.16	0.24	0.14
standard deviation	EdR GCM	0.22	0.26	0.21	0.20	0.26	0.18	0.21	0.13

Table 5. Times during which the 5-decade running mean temperature reconstructed by Wang et al. (1998) is above the "pre-industrial noise level", given by mean plus 2 standard deviation for the time 1590-1910.

Region	times with significantly elevated temperatures
1	1920-1980
2	1930-1980
3	1930-1970
4	1950-1980
5	1930-1980
6	1940-1960
7	1920-1980
8	1920-1980

The times when the reconstructed temperature is beyond the 1590-1910 average plus 2 standard deviations are listed in Table 5, with the parameters given in Table 4. On average, about 98% of all pre-industrial temperatures should be below this level. In fact, this estimate of the pre-industrial noise level is conservative, as all temperatures were beyond this level (Figure 5). This is due to the skewing of the temperature distribution.

In all 8 regions, most of the twentieth century temperatures were above the pre-industrial noise level, as defined by either the CC model data or Wang et al.'s reconstructions (Figure 5). If the standard deviations derived from Wang's reconstruction are replaced by the larger standard deviations derived from the pre-industrial periods in the GCM simulations, similar noise levels are obtained (Figure 5) with the same overall conclusions, namely that during most of the

twentieth century the reconstructed temperatures are significantly elevated compared to the pre-industrial period 1590-1910.

Thus, we conclude that the recent warming in China, as it is documented in Wang et al.'s (1998a) reconstruction, is beyond the range of natural variation, and that an explanation of the phenomenon requires the consideration of other factors, in particular increased levels of atmospheric greenhouse gas concentrations.

Attribution

In order to assess the likelihood that greenhouse gas forcing would be responsible for the recent warming; a simple statistical model for the temperature evolution is fitted to the output of the GCM simulation for each of the eight boxes:

$$(*) \quad T_{t+1} = \alpha T_t + \beta S_t + \gamma \log(C_t) + n_t$$

Here, T_t is the smoothed temperature deviation from the pre-industrial mean (1590-1910; given in Table 4); S_t is the time-variable solar forcing deviation from the pre-industrial mean 1590-1910, and C_t the time variable deviation in greenhouse gas concentrations, n_t stands for the remainder which is consider in this context as noise. The coefficients α, β, and γ are determined so that the model variations are best described:

Table 6. Regional coefficients of the model.

Region	α	β	γ
1	0.604	0.118	1.697
2	0.643	0.087	1.562
3	0.867	0.009	1.365
4	0.740	0.039	1.272
5	0.709	0.064	1.443
6	0.962	-0.008	1.351
7	0.714	0.040	1.306
8	0.836	0.043	1.456

A direct comparison of the three parameters is not possible since the variance of the temperature itself and of the two forcing factors is different. However, the memory term αT_t is the most important – the very magnitude of α is due to the heavy smoothing by the 5-decade running mean filter. The influence of the solar forcing varies substantially between the 8 regions, and in one case the fit even results in a physically implausible negative value – indicating that the fit may suffer somewhat form estimation problems. The parameter γ-coefficient is similar in the eight boxes.

The model is linear, so that sum of the response T_t^s to solar and volcanic forcing alone and of the response T_t^c to greenhouse gas forcing alone equals the response to both forcings, if the noise is disregarded and both are integrated with the same initial value T_{1590}. Therefore,

equation (*) allows an estimate of the relative importance of the two forcing factors. In following table 7, we list the reconstructed change of temperature according to Wang et al. (1998a), the change estimated through (*) to solar and volcanic forcing alone, to greenhouse gas forcing alone, and to both of them. These are all deviations from the pre-industrial values (1590-1910)

Table 7. Reconstructed change of temperature according to Wang et al. (1998a), the change estimated through (*) to solar and volcanic forcing alone, to greenhouse gas forcing alone, to both forcings, and the ratio of Wang to (*). These are all deviations from the pre-industrial values (1590-1910).

Region	1	2	3	4	5	6	7	8
Wang et al. (1998a)	0.47	0.49	0.36	0.28	0.50	0.47	0.81	0.70
(*) with S_t=0	0.48	0.47	0.69	0.47	0.50	0.72	0.69	0.45
(*) with log C_t=0	0.59	0.45	0.04	0.23	0.38	-0.18	0.31	0.23
(*) with both forcings	1.08	0.93	0.73	0.70	0.88	0.58	1.00	0.68
Ratio Wang/(*)	0.44	0.53	0.49	0.40	0.57	0.81	0.81	1.02

When comparing the historical warming with the estimated warming (second and fifth rows) we find that (*) gives higher values. The ratio of the two numbers (last row) varies between 0.40 in the eastern part of China and 1.02 in the western part. We suggest that this overestimation by model (*) reflects the increasing cooling effect of regional emissions of industrial aerosols, which are strongest in the densely populated east and south of China, while the western part of China experiences less increasing emissions.

Apart from region 1, the estimated warming due to solar and volcanic effects (fourth row) is smaller than the estimated anthropogenic greenhouse effect (third row). Only the anthropogenic greenhouse effect is strong enough to explain the observed warming, in spite of the fact that the latter is considerably reduced by the unaccounted-for effect of the increasing industrial aerosol impacts.

We conclude that the total estimated response is consistent with the empirical evidence in terms of sign and, to a lesser extent, with magnitude. The major part of the twentieth century warming can be explained only with the help of the anthropogenic greenhouse gas effect, whereas the solar effect can account for only a smaller proportion. Differently from the development in the GCM simulations, which is a steady upward trend throughout the twentieth century, there is in the reconstructions a decline in the second half of the twentieth century. We suggest that this is reflecting the steady increase of industrial aerosol emissions (Krüger, pers. communication) in China.

Conclusions

We have analyzed Wang et al.'s (1998a) reconstruction of regional temperatures in China since the sixteenth century with respect to traces of the impact of changing forcing conditions. We found that the reconstructed temperatures are reasonably well simulated by a climate model subject to time-variable solar, volcanic and greenhouse gas forcing. The similarity is good on time scales of a century, while the model generates variability on shorter time scales without a counterpart in the reconstructions.

The development of regional temperature in the recent decades of the industrial period is towards significantly elevated levels, where the significance is assessed by comparison against a

pre-industrial “normal” and “noise level”. Thus, the presence of non-normal external factors must be assumed. Using the GCM simulations to assess the relative importance of the solar, volcanic, and greenhouse gas forcing, we find that only the greenhouse gas forcing can account for the recent warming.

There are a number of potential sources for errors. The most severe is the reliability of the historical reconstructions of regional temperature in China. These temperatures are rather uncertain not only because of the usual uncertainties in data derived from, for instance, tree ring width, but also since the data base of instrumental data to build the empirical transfer functions is not good. Other caveats refer to the model simulations. For instance, the inclusion of the volcanic effects is relatively rough. Also, the effect of industrial aerosols of cooling the regional atmosphere is not represented in the model simulations. Finally, the utilized forcing factors suffer from uncertainties.

Acknowledgements

Financial support was provided by the Natural Sciences Foundation of China (40272123), the Chinese Academy of Sciences (KZCX3-SW-321) and by the GKSS Research Center in Geesthacht, Germany. Valuable help and advice were given by Fidel Gonzàlez-Ruoco and Olaf Krüger. Beate Gardeike helped professionally with the diagrams.

References

Blunier, T., J.A. Chappellaz, J. Schwander, B. Stauffer, and D. Raynaud, 1995. Variations in atmospheric methane concentration during the Holocene epoch. *Nature* 374, 46-49.

Crowley, T.J., 2000, Causes of climate change over the past 1000 years. *Science* 289, 270-277.

De Zolt, S., P.Lionello, J. Luterbacher and E. Zorita, 2003. The variability of the winter European climate and the NAO index during the last 500 years. (in preparation)

Etheridge D., L.P Steele, R.L. Langenfelds, R.J. Francey J.M. Barnola, V.I., Morgan, 1996. Natural and anthropogenic changes in atmospheric CO2 over the last 1000 years from air in Antarctic ice and firn. *J. Geophys. Res.* 101, 4115-4128.

González-Ruoco, J.F., H. von Storch and E. Zorita, 2003. Deep soil temperature as proxy for surface air-temperature in a coupled model simulation of the last thousand years . *Geophys. Res. Lett.* 30, 2116-2125.

Hasselmann, K., 1979. On the signal-to-noise problem in atmospheric response studies. *Meteorology over the tropical oceans*, B.D. Shaw ed., Roy. Metorol. Soc., Bracknell, Berkshire, England, 251-259.

Hegerl, G.C., K.H. Hasselmann, U. Cubasch, J.F.B. Mitchell, E. Roeckner, R. Voss and J. Waszkewitz, 1997. Multi-fingerprint detection and attribution analysis of greenhouse gas, greenhouse gas-plus-aerosol and solar forced climate change. *Clim. Dyn.* 13, 613-634.

Jones, P.D., M. New, D.E. Parker et al. 1999. Surface air temperature and its changes over the past 150 years. *Rev. Geophys.* 37, 173-199.

Legutke, S., and R. Voss, 1999, The Hamburg atmosphere-ocean coupled circulation model ECHO-G. *Technical Report No. 18*, DKRZ, Hamburg, Germany.

Liu, H-B. and X-M. Shao, 2002. Reconstruction of the dry index series of early summer during the last 500 years within the Pass area of Shaanxi of China and adjacent area. *Quaternary Sciences* 22 (3), 220-229 (in Chinese).

Liu, Y. and Q-F. Cai, 2002. Tree ring precipitation records and changing of eastern Asian summer monsoon — Taking Baotou area of the Inner Mongol as an example. *Front of Earth Sciences* 8 (1), 91-97 (in Chinese).

Liu, Y. and L-M. Ma, 1999. Reconstruction of seasonal precipitation from tree ring width of Huhehaote during the last 376 years. *Chinese Sci. Bull.* 44 (18), 1986-1992 (in Chinese).

Wang, Sh-W., J-L. Ye, and Gong D-Y, 1998a. Climate of Little Ice Age in China. *Quaternary Sciences* 18 (1), 54-64 (in Chinese).

Wang, Sh-W., J-L. Ye, D-Y. Gong, J-H. Zhu, and T.D. Yao, 1998b. Construction of mean annual temperature series for the last one hundred years in China. *Quart. J. Appl. Meteorol.* 9 (4), 392-401 (in Chinese).

Wang, Sh-W, Gong D-Y, 2000, Temperatures of China in several typical periods of Holocene. *Prog. Nat. Sci.* 10 (4), 325-332 (in Chinese)

Xu, J-H., 1998. Sun, climate, famine and national migration. *Science in China (series D)*, 41 (5), 449-472.

Yang B., et al., 2002. Research progress on climate change during the last 2000 years. *Progress in Earth Science* 17 (1), 110-117 (in Chinese).

Yao, T-D, D-H. Qin, L-D. Tian, et al., 1996. Variations in temperature and precipitation in the past 2000a on the Tibetan Plateau: Guliya ice core record. *Science in China (series D),* 39 (4), 425-433.

Zheng, J-Y, and Zheng S-Zh, 1993, States of cold, warm, drought and waterlogging of Shandong province during historical period. *Journal of Geography*, 48(4) 348-357 (in Chinese)

Zinke, J., H. von Storch, B. Müller, E. Zorita, B. Rein, H. B. Mieding, H. Miller, A. Lücke, G.H. Schleser, M.J. Schwab, J.F.W. Negendank, U. Kienel, J.F. González-Ruoco, C. Dullo and A. Eisenhauser, 2004, *Evidence for the climate during the Late Maunder Minimum from proxy data available within KIHZ.* In H. Fischer, T. Kumke, G. Lohmann, G. Flöser, H. Miller, H, von Storch und J. F. W. Negendank, eds., *The KIHZ project: Towards a synthesis of Holocene proxy data and climate models*, Springer Verlag, Berlin, in press.

Zorita, E., H. von Storch, F. González-Rouco, U. Cubasch, J. Luterbacher, S. Legutke , I. Fischer-Bruns and U. Schlese, 2003, *Simulation of the climate of the last five centuries*, GKSS Report 2003/12, 43 pp.

Zwiers, F., 1999. The detection of climate change. In: H. von Storch and G. Flöser, eds., *Anthropogenic Climate Change*, Springer Verlag, Berlin, 163-209.